Journal of Analytical and Applied Pyrolysis 192 (2025) 107295

Contents lists available at ScienceDirect

Journal of Analytical and Applied Pyrolysis

journal homepage: www.elsevier.com/locate/jaap

Explicit microrelief-controlled decoupling of initial aerobic decay and leaching (in hummocks) and anaerobic decay (in hollows) in surface layers of a *Sphagnum*-dominated peatland

M. Pérez-Rodríguez [a], A. Alten [a], M. Miler [b], J. Kaal [a,c,*]

[a] Institut für Geoökologie, AG Umweltgeochemie, Technische Universität Braunschweig, Braunschweig, Germany
[b] Geological Survey of Slovenia, Ljubljana, Slovenia
[c] Pyrolyscience, Santiago de Compostela 15707, Spain

ARTICLE INFO

Keywords:
Py-GC-MS
THM-GC-MS
Peat
Organic matter
Polysaccharides
Sphagnum acid

ABSTRACT

Understanding decay processes in peat deposits is fundamental for predicting their role as sources or sinks of atmospheric carbon in a changing environment. It is known that the distribution of microhabitats –hummock, lawn and hollow– within peatlands affects organic matter quality and degradation, but microtopography-dependent carbon dynamics are poorly understood on the molecular level. We studied early decomposition across microtopography levels through analyses of superficial moss cores from a *Sphagnum*-dominated ombrotrophic peatland in Central Germany, and a 400-day incubation experiment, using analytical pyrolysis. Interpretations were aided by analysis of living vegetation and a deep peat core as reference. Stable and labile pools of polysaccharides dominated the pyrolyzates and played a crucial role in decay dynamics. Two distinct degradation processes emerged: 1) anaerobic decay, characterized by loss of polysaccharides and selective preservation of lignin and aliphatic OM; and 2) leaching of labile phenolic compounds (including sphagnum acid) and free carbohydrates with concomitant initial aerobic degradation and selective preservation of structural polysaccharides. The relative importance of these initial decay processes is spatially dependent; anaerobic decay was detectable in only some of the more evolved hollow layers, while aerobic degradation and leaching dominated in hummocks. Sphagnum acid's molecular markers appeared useful tracers of early decay as it probably has a leaching-sensitive component in hyaline cells (corroborated by SEM micrographs) that is lost rapidly from hummocks, but not from hollows. Hence, the occurrence of sphagnum acid in peat cores is influenced by microrelief position during peat accretion. This study highlights how microhabitat variations within peatlands influence decay mechanisms on the molecular level.

1. Introduction

Peatlands store 530 ± 160 Pg of organic C globally [1], constituting a long-term global sink of atmospheric CO_2. In northern peatlands, which are currently subjected to very rapid climate change [2], bryophytes dominated by the genus *Sphagnum* comprise ~45 % of the total accumulated peat [3]. These "peat mosses" are adapted to the acid, cool, waterlogged and oligotrophic conditions, which they create and maintain, and are considered vital for C persistence and accumulation [4]. It is known that the accumulation of polysaccharides of the cell walls of *Sphagnum* tissues plays an important role in the overall slow C mineralization in comparison to the litter of other bryophytes [5]. However, on the molecular scale, factors driving moss decay rates in *Sphagnum*-dominated peatlands, and in particular the interplay between decay rates and microscale variations in relief and vegetation composition, remain unclear [6].

Several studies have shown differences in decomposition rate and litter characteristics between microhabitat levels in *Sphagnum*-dominated peatlands such as hummock and hollow [7–9]. The decay of hummock species (e.g. *S. fuscum*) tends to be slower than that of the species that dominate wetter hollow microtopographic levels such as *S. cuspidatum* [7–12]. Furthermore, *Sphagnum* mosses show a trade-off between OM decay and growth capacity: fast-growing species –mainly hollow species– exhibit faster decay than the more decay-resistant slower growing species in the hummock [9,10,13]. Species such as *Polytrichum strictum* can outcompete other mosses in dry spots in

* Corresponding author at: Institut für Geoökologie, AG Umweltgeochemie, Technische Universität Braunschweig, Braunschweig, Germany.
E-mail address: joeri@pyrolyscience.com (J. Kaal).

https://doi.org/10.1016/j.jaap.2025.107295
Received 22 March 2025; Received in revised form 24 June 2025; Accepted 17 July 2025
Available online 18 July 2025

northern peatlands such as hummock, due to their drought tolerance [14]. The role of the different traits of hummock and hollow species in OM decomposition, especially on the molecular scale, have barely been explored.

Sphagnum species have idiosyncratic physiological, anatomical and molecular features, which affect the decay of their tissues [15,16], and this is the main reason why molecular-based approaches are required to improve our understanding of OM dynamics in *Sphagnum*-dominated peatlands. Firstly, the leaves of *Sphagnum* moss consist of photosynthetic cells (chlorophyllose cells or chlorocytes) and specialized hyaline cells (hyalocytes). These hyaline cells are large, dead, porous cells with an extraordinary water absorbing capacity that contain N-fixating cyanobacteria, other microorganisms and metabolites [17,18]. They can account for 90 % of the volume of *Sphagnum* tissues [19]. The capacity of *Sphagnum* to create and maintain acidic conditions has been attributed to hyaline cell constituents such as uronic acids [16,20], present both in dissolved state and in cell walls as a pectin-like structural polysaccharide known as sphagnan [16,21], which can be released post-mortem from hyaline cells as well [16]. Secondly, another metabolite, sphagnum acid, i.e. *p*-hydroxy-β-(carboxymethyl)-cinnamic acid [16,22], is a phenolic compound that is unique of *Sphagnum* spp. that has been associated with the slow decomposition of *Sphagnum* moss tissues [15,23,24] even though several molecular-based studies indicate otherwise [6,25]. Studies that pinpoint the role of these enigmatical *Sphagnum* moss constituents during early decay of hummock and hollow materials are needed to improve our understanding of peat formation. Analytical pyrolysis techniques are suitable for achieving these objectives [26], but studies using them to determine early decay of *Sphagnum*-dominated moss communities by multicore semi-quantitative analyses are lacking.

We studied the early stages of moss-derived OM degradation and its conversion into peat at the microhabitat level, aiming to determine the role of peatland microtopography in carbon accumulation and improve our understanding of molecular proxies of peat degradation that are commonly used in paleo-environmental reconstruction of historical water tables and decomposition dynamics. For this purpose, we analyzed samples from superficial moss cores (15–50 cm deep) and set up a 400-days *in-vitro* (mesocosm) decomposition experiment of the layers in these cores, followed by analytical pyrolysis for molecular assessments. We hypothesized that 1) the initial stage of organic matter decomposition depends on microhabitat due to differences in oxygen conditions, 2) the different biomolecular constituents decay at different rates depending on aerobic decay, anaerobic decay, and leaching, and 3) early degradation of *Sphagnum* materials is controlled by leaching from hyaline cells with consequent effects on molecular composition.

2. Materials and methods

2.1. Sample collection, processing and incubation experiments

The Odersprung bog (52°46.383' N, 10°33.816' E; 800 m a.s.l.) is a 27.5 ha ombrotrophic peatland located within the Nationalpark Harz nature reserve in the Harz Mountains (Central Germany; Fig. 1). It is classified as a saddle bog forming the watershed between the Oder and Bode streams. The mean annual precipitation and temperature are 1264 mm and 5.9 °C, respectively. The vegetation consists mainly of bryophytes especially *Sphagnum* spp., as well as *Carex rostrata*, *Molinia caerulea*, *Calluna vulgaris* and *Eriophorum angustifolium* [27]. Among the peat moss species, *S. magellanicum* associated with *S. rubellum* dominates while the association between *S. magellanicum* and *S. papillosum* is also abundant. Other bryophytes are *Polytrichum* (*P. commune* and *P. strictum*) and *S. cuspidatum*.

Superficial cores of moss materials (15–50 cm), consisting of naturally occurring mixtures of *Sphagnum* and *Polytrichum* species, were collected in June 2019 using a ceramic knife at two locations about 50 m

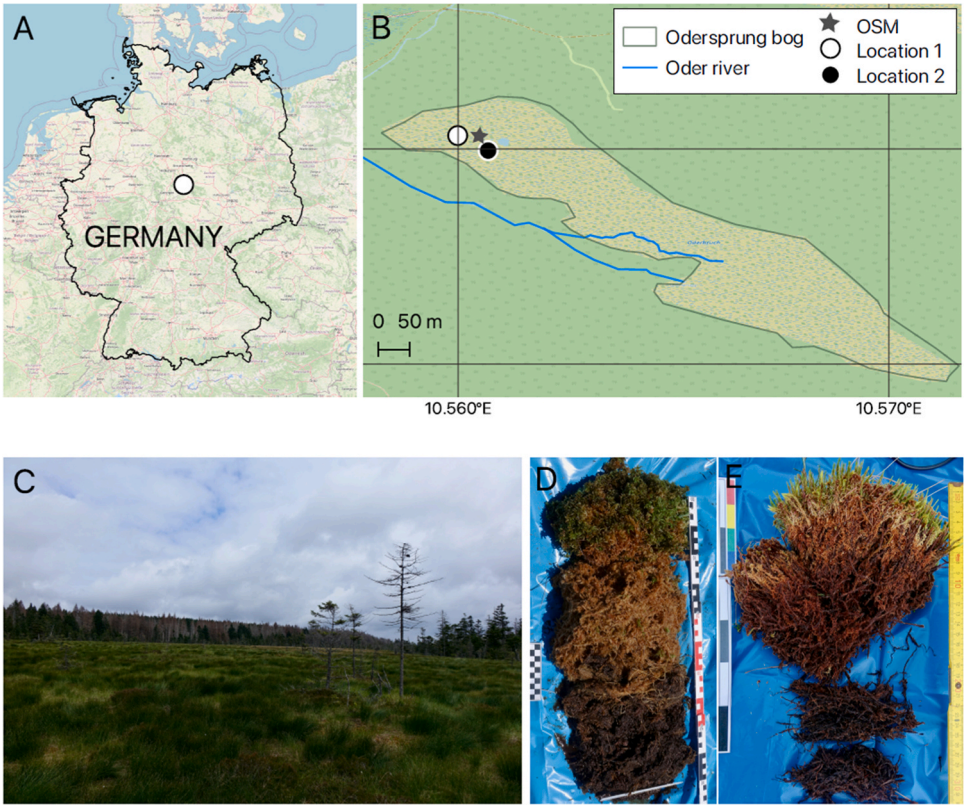

Fig. 1. Characteristics of the study area. a) Location of the Harz National Park in Central Germany (OpenStreetMap); b) location of the Odersprung bog, with the sampling locations 1 (from which the HU-1 and HO-1 cores were obtained), location 2 (HU-2 and HO-2) and of the 3 m deep peat core (OSM core). The Oder river (peatland outflow) is also shown. c) Picture of the Odersprung bog facing southeast; d-e) Pictures of two collected cores, HO-2 (d) and HU-2 (e).

apart (Fig. 1). At the time of sampling, the water table was high, resulting in waterlogged hollows and lawns, with hummock surfaces up to around 15 cm above the water table. Nevertheless, conditions before sampling include the severe 2018 drought in Northern and Central Europe [28]. At each location, two different microhabitats –hummock and hollow– were sampled at a distance of 1–5 m. The four superficial cores (two hollow and two hummock cores) consisted of mostly living vegetation and senescent moss, as well as the first peat layer (Table 1). The upper section of the cores consisting of "fresh" plant material, i.e. green-coloured moss including the capitulum, was denoted (Table 1).

Samples of the surface cores (1.3–6.5 g dry weight, aiming for similar sample volumes) were incubated *in vitro* following the procedure described in Bengtsson et al. [10]. Liverworts, roots and rhizomes were removed from the litter by hand, which was then dried at 60°C until constant weight. Next, the samples were added to an acid-cleaned nylon mesh bag. The bags were placed into amber jars covered with perforated lids to minimize evaporation while allowing air exchange. Samples were kept at room temperature (~20 °C) in an inoculum containing deionized water and nutrients to avoid nutrient limitation during decomposition [6], in addition to microorganisms from the peatland. These microorganisms were water-extracted from the surface (0–15 cm) of the same bog area, following Hájek et al. [6]. Shortly, approximately 1 kg of fresh litter was shaken in 3 L deionized water for 1 h. The slurry was then filtered through a polyamide mesh and filter paper. The mesocosms were shaken regularly to increase oxygen availability and ensure contact between the sample and the inoculum. The nutrient solution was replenished three times during the first 200 days of the experiment. Total incubation time was 400 days. Subsamples were obtained after 200 (t_{200}) and 400 (t_{400}) days. Samples were rinsed in deionized water and dried before analysis. To obtain information of the physical status of the mosses, selected samples (core HO- 2 hollow samples from 0 to 15 cm and 15–30 cm depth) were also examined by scanning electron microscopy (SEM) in secondary electron mode at 20 kV accelerating voltage and 48 spot size using a JEOL JSM-6490LV.

We sampled living moss from the same bog area, including peatland mosses (*Sphagnum cuspidatum*, *S. magellanicum*, *S. papillosum*, *S. capillifolium*) and haircap mosses (*Polytrichum commune* and *P. strictum*). The objective of including these reference materials was to identify the species-specific molecular fingerprints.

A 3 m deep Odersprung bog core (referred to as OSM core) was obtained in October 2018 in a flat ("lawn") area between two locations where a hummock-hollow pair of short cores was collected. The upper meter of the core was collected using a Wardenaar corer whereas deeper sections were taken using a peat borer. Living vegetation was excluded. The core was sliced into 5 cm sections in the laboratory, of which six samples were included in the present study (0–5, 5–10, 10–15, 15–20, 50–55 and 295–300 cm, Table 1). The samples were preserved at 4 °C until drying at 40 °C to constant weight. The OSM core was included to facilitate the recognition of molecular effects of anaerobic decay, which is much more intense for deeper peat material than for the superficial moss cores.

2.2. Analytical pyrolysis

Dried samples were milled to a fine powder with an agate ball mill (MM40, Retsch GmbH, Haan, Germany). Pyrolysis-GC–MS was performed on all samples ($n = 57$; Table 1) using a CDS Pyroprobe coupled to an Agilent Technologies 5977 GC–MS. Samples were embedded in glass wool-containing quartz tubes and pyrolyzed at 650 °C set-point temperature for 20 s (heating rate 10 °C/ms). The pyrolysis-GC interface, GC inlet, and GC–MS interface were set at 325 °C. The GC was equipped with a HP-5MS (5 % phenyl, 95 % dimethylpolysiloxane)

Table 1
List of samples included in this study and availability of molecular characterization data. Non-incubated samples are indicated as t0 and incubated samples as t200 (200 days) or t400 (400 days). The "upper depth" column indicates the depth of the upper part of the study samples; the total thickness is part of the "description' column". For capitulum samples (parts that emerge several centimetres above the moss surface), the upper depth is indicated as −5 cm.

Lab code	Description	Origen	Core	Upper depth	Py-GC-MS			THM-GC-MS		
				(cm)	t0	t200	t400	t0	t200	t400
H0524	HO−1 capitulum	Hollow	HO−1	−5	v	v	v	v	v	v
H0525	HO−1 0–10 cm	Hollow	HO−1	0	v	v	v	-	-	-
H0526	HO−1 10–15 cm	Hollow	HO−1	10	v	v	v	-	-	-
H0541	HO−2 capitulum	Hollow	HO−2	−5	v	v	v	v	v	v
H0542	HO−2 0–15 cm	Hollow	HO−2	0	v	v	v	v	v	v
H0543	HO−2 15–30 cm	Hollow	HO−2	15	v	v	v	-	-	-
H0547	HO−2 30–40 cm	Hollow	HO−2	30	v	v	v	v	v	v
H0548	HO−2 40–50 cm	Hollow	HO−2	40	v	v	v	v	v	v
H0531	HU−1 0–15 cm (green)	Hummock	HU−1	0	v	v	v	-	-	-
H0532	HU−1 0–15 cm (brown)	Hummock	HU−1	5	v	v	v	v	v	v
H0533	HU−1 15–25 cm	Hummock	HU−1	15	v	v	v	v	v	v
H0534	HU−1 25–30 cm	Hummock	HU−1	25	v	v	v	-	-	-
H0535	HU−1 > 30 cm	Hummock	HU−1	30	v	v	v	v	v	v
G0959	HU−2 0–4 cm (green)	Hummock	HU−2	0	v	-	-	-	-	-
G0960	HU−2 0–4 cm (brown)	Hummock	HU−2	0	v	-	-	-	-	-
G0963	HU−2 4–9 cm	Hummock	HU−2	4	v	-	-	-	-	-
G0966	HU−2 9–20 cm	Hummock	HU−2	9	v	-	-	-	-	-
G0961	HU−2 20–25 cm	Hummock	HU−2	20	v	-	-	-	-	-
G0962	HU−2 25–28 cm	Hummock	HU−2	25	v	-	-	-	-	-
OSM05	OSM−0–5*	Lawn	OSM	0	v	-	-	v	-	-
OSM510	OSM−5–10*	Lawn	OSM	5	v	-	-	v	-	-
OSM1015	OSM−10–15*	Lawn	OSM	10	v	-	-	v	-	-
OSM1520	OSM−15–20*	Lawn	OSM	15	v	-	-	v	-	-
OSM5055	OSM−50–55*	Lawn	OSM	50	v	-	-	v	-	-
OSM300	OSM−295–300*	Lawn	OSM	295	v	-	-	v	-	-
P1	*S. magellanicum**	Sphagnum	-	-	v	-	-	-	-	-
P2	*S. papillosum**	Sphagnum	-	-	v	-	-	-	-	-
P3	*S. capillifolium**	Sphagnum	-	-	v	-	-	-	-	-
P4	*P. strictum**	Polytrichum	-	-	v	-	-	-	-	-
P5	*P. commune**	Polytrichum	-	-	v	-	-	-	-	-
P6	*S. cuspidatum**	Sphagnum	-	-	v	-	-	-	-	-

* samples included in this study as reference materials of a deep peat core (OSM) and Sphagnum and Polytrichum mosses.

column (length 30 m; i.d. 0.25 mm; film thickness 0.25 μm). Helium was used as carrier gas (constant gas flow, 1 ml/min, split mode 1:25). The GC oven was heated from 50 to 325 °C at 20 °C/min with a 3 min final hold. The ion source of the MS operated in electron impact mode (70 eV) at 230 °C and the quadrupole detector was held at 150 °C, measuring fragments in the *m/z* 50–500 range. Relative proportions of the pyrolysis products were calculated as the percentage of the total quantified peak area, using the peak areas of the main fragment ions (*m/z*) of each product.

Thermally-assisted Hydrolysis and Methylation (THM-GC-MS) was done on a reduced number ($n = 30$; Table 1) of samples to understand trends in Py-GC-MS fingerprints of those OM constituents for which THM-GC-MS has a better structure-resolving capacity, in particular that of sphagnum acid. For this purpose, tetramethylammonium hydroxide reagent (TMAH, 25 % in water, from Sigma-Aldrich) was added to sample-containing quartz tubes, assuring that the solution completely soaked the sample, and then inserted into the pyrolysis interface after no less than 30 min. GC-MS conditions were similar to those of Py-GC-MS, with exception of a 4 min initial hold at 70 °C (solvent delay period) and a split ratio of 1:50.

2.3. Data evaluation

Molecular data interpretation was based on relative proportions of individual compounds, compound groups and proxies of decay processes [29–32]. Furthermore, for Py-GC-MS only, principal components analysis (PCA) was performed for dimensionality reduction of the 123 attributes (proportions of each individual pyrolysis product), without applying rotations, using Tanagra 1.4 software. Other statistical analyses included linear correlation analysis, Pearson correlation, the one-sample *t*-test and one-way analysis of variance (ANOVA), using SPSS and R Core Team [33] software packages. More specifically, to assess differences among 1) microhabitats (hollow, hummock, OSM peat), 2) between paired cores (HO-1 vs. HO-2; HU-1 vs. HU-2) and 3)

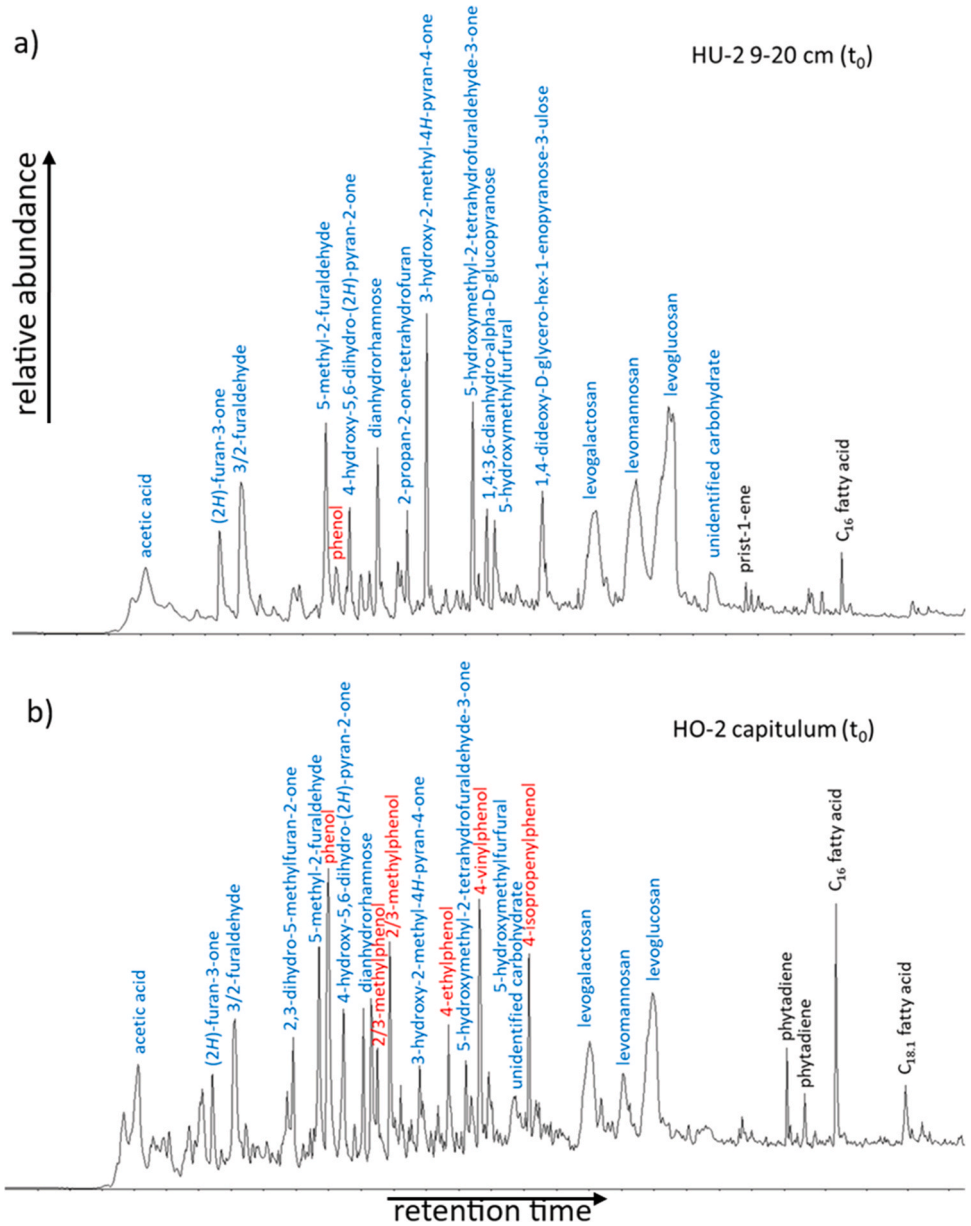

Fig. 2. Example total ion chromatograms from pyrolysis-GC-MS of a) a polysaccharide-dominated hummock sample (HU-2 core, 9–20 cm depth, not incubated) and b) the more diverse fingerprint of the capitulum of the core HO-2 hollow sample (not incubated). Carbohydrates are indicated in blue, phenolic compounds in red and long-chain aliphatic compounds in black font.

across incubation times for pyrolysis and THM products, we first evaluated the assumptions of normality (Shapiro-Wilk test, applied to each group) and homoscedasticity (Levene's test). Variables meeting both criteria were analysed by one-way ANOVA followed by Tukey's *post-hoc* test. Where either assumption was violated, we applied nonparametric methods; the Kruskal–Wallis test with subsequent paired comparisons using the Wilcoxon test. An α threshold of 0.05 was applied for all the analyses.

3. Results

3.1. Product source assessment and main trends

3.1.1. Py-GC-MS

Carbohydrate products dominated the pyrolyzates, accounting for 78.5 % (mean) ± 9.8 % (standard deviation) of total quantified signal (Supplementary Dataset; Fig. 2). In decreasing order of average proportion, the main carbohydrate products [34] were levoglucosan, 3/2-furaldehyde, levogalactosan, 5-methyl-2-furaldehyde, acetic acid and levomannosan, potentially derived from structural polysaccharides (holocellulose, sphagnan) and free low molecular weight carbohydrates. The hummocks had a significantly larger carbohydrate proportion than the hollow cores (84 % vs. 75 %) (Fig. 3a). The ratio of levoglucosan to total carbohydrates (Lglu/Ps), a potential proxy of polysaccharides preservation state [31,32], increased with depth in the OSM peat core (Fig. 3b).

Most of the remaining signal corresponded to phenolic products (11.7 ± 6.2 %) that were classified into several subgroups. The guaiacols (G-type; 1.6 ± 1.9 %) and syringols (S-type; 0.6 ± 0.9 %) are characteristic products of lignin in vascular plant tissues [35]. The hollows produced larger proportions of these G- and S-type products than the hummocks ($P < 0.001$; Fig. 3c/3d). Phenolic products based on the *p*-hydroxyphenyl moiety (H-type) –4-vinylphenol, 4-propenylphenol, 4-hydroxybenzoic acid and 4-methyl-2-phenylphenol (2.1 ± 1.3 %)– probably originated from a combination of lignin, *p*-coumaric acid and *p*-hydroxybenzoic acid-acylated lignin [36]. *Sphagnum* species produced much more ($P < 0.001$) H-type products (3.3–4.1 %) than *Polytrichum* species (0.2–0.7 %) (Supplementary Dataset), corroborating the relatively high yields of H-type products after pyrolysis of *Sphagnum* [36,37], and of hollows rather than hummocks ($P < 0.001$; Fig. 3e). Formed upon decarboxylation of sphagnum acid [23,38,39], 4-isopropenylphenol (4IPP; 0.9 ± 0.6 %) was allocated to a separate subgroup. Among the fresh moss samples, 4IPP was detected only in *Sphagnum* (1.9–2.9 %; Supplementary Dataset). It was more abundant ($P < 0.001$) in hollows than in hummocks (Fig. 3f). In hummocks, only the superficial fresh tissues (capitulum and green-coloured moss) had a 4IPP yield in the range of living moss samples (almost 2 %) (Supplementary Dataset). In the OSM peat core, 4IPP decreased from 1.7 % at 0–5 cm to 0.2–0.6 % below that depth (Fig. 3f). Finally, phenol and C_1-C_2-alkylphenols (6.6 ± 3.9 %) can originate from many sources, but in the present sample set, where protein and true lignin products were scarce, they were likely derived from unspecified moss phenolics and H-type lignin monomers [40]. Both (alkyl)phenols and H-type products decreased relatively with depth in the OSM peat deposit (Fig. 3g).

Many compounds based on polymethylene chains (MCC) were detected, including alkanes, alkenes, fatty acids, methylketones, N-containing MCC (alkylnitriles and -amides) and phytadienes from chlorophyll (3.7 ± 2.6 %). The MCC were much more abundant in deeper (>10 cm) reference peat samples than in the superficial moss core materials (Fig. 3h).

Other compounds with nitrogen, such as pyrroles, pyridine, indoles and diketopiperazines (1.7 ± 0.8 %; Fig. 3i), originated predominantly from proteins [41]. The aromatic products benzene and toluene accounted for 2.2 ± 1.5 % (Fig. 3j). Toluene increased with depth in the OSM peat deposit, indicating it is mainly associated with degraded OM [42] (Supplementary Dataset).

Differences in molecular composition between the four *Sphagnum* species were small (Supplementary Dataset). The linear correlation coefficients of the compound categories of all species' combinations exceeded $r = 0.98$ ($P < 0.001$), and for the two *Polytrichum* species as well ($r = 0.97$; $P < 0.001$). ANOVA comparing *Sphagnum* and *Polytrichum* showed no significant difference in compound class proportions except for the aforementioned differences in H-type phenols and obviously 4IPP, which were more abundant in the *Sphagnum* mosses.

3.1.2. THM-GC-MS

The three main groups of THM products were carbohydrate products (27.1 ± 5.8 %), methoxybenzene-based products of polyphenols including lignin, sphagnum acid and tannin (30.7 ± 5.7 %) and polymethylene-based products (MCC; 26.2 ± 6.4 %) (Supplementary Dataset). The carbohydrate products –mostly methylated C_5- and C_6-metasaccharinic acids [43–45]– are underrepresented because mainly free (or terminal) carbohydrates are released due to inefficient hydrolysis under alkaline conditions of the TMAH reagent [46]. Nevertheless, the THM-GC-MS dataset probably represents a meaningful part of the OM, as shown by the strong correlation in relative proportions of sphagnum acid products between the two pyrolysis techniques (r^2=0.80; $P < 0.001$).

The phenolic products included a large proportion of H-type products (10.3 ± 3.5 %) compared to G- (8.4 ± 3.7 %) and S-type (2.5 ± 1.6 %) compounds, typical of THM fingerprints of *Sphagnum*-dominated peat [47], and indicative of predominance of non-lignin phenolics to the H-type products. Sphagnum acid was recognized by 4-isopropenylmethoxybenzene and three 3-(4-methoxyphen-1-yl)butenoic acid methyl ester products [23,48]. As for 4IPP from Py-GC-MS, these products showed a drastic relative decrease from the surface (10 %) to 5–10 cm depth (2 %) in the OSM deposit (Fig. 3k). The ratio of isopropenyl to butenoic acid side chain ratios among *Sphagnum* markers (4-isopropeneylphenol/(*cis*- + *trans*-3-(4′-methoxyphen-1-yl)but-2-enoic acid methyl ester + 3-(4′-methoxyphen-1-yl)but-3-enoic acid methyl ester)(Fig. 3l), which indicates sphagnum acid decay [30], increased with depth. As for Py-GC-MS, the hollow samples were enriched in THM products of sphagnum acid (sum and all individual markers) and H-type products (Supplementary Dataset) compared to the hummocks. The 1,3,5-trimethoxybenzenes increased with depth in the OSM deposit, which may represent the poorly understood condensed tannin-like phenolic ingredient in *Sphagnum* [29,49,50]. The hummock samples were enriched in these tannin or tannin-like products (Supplementary Dataset).

The fatty acids (detected as methyl esters; FAMEs) included methylated unsubstituted C_{14}-C_{30} FAMEs, *iso-/anteiso*-C_{15} FAME, mid-chain substituted di- and trimethoxy-C_{16}- and -C_{18} FAMEs, ω-methoxy FAMEs (C_{16}-C_{24}) and diacids (DAMEs; C_{16}-C_{28}), from epicuticular waxes, cutin and suberin [16,51,52]. Some fatty acids (C_{14}, C_{15}, *iso/-anteiso* C_{15}, $C_{18:1}$, C_{30}) were more abundant in hummocks than in hollows ($P < 0.05$) (Supplementary Dataset).

3.2. Principal components analysis (PCA)

Two principal components (PC1 and PC2) accounted for 50 % of total variance in the Py-GC-MS dataset. The lignin (G- and S-type) products and MCC had high positive loadings (>0.7) on PC1 (Fig. 4a), which had an eigenvalue of 42.9 and explained 35 % of variance. None of the products have high negative loadings (<-0.7). All samples below 0–5 cm from the OSM core had positive PC1 scores (Figs. 4b,4c). The samples from extant mosses and surface cores had low negative scores with several exceptions of hollow samples, in particular the deepest samples corresponding to the first peat layer of core HO-1.

PC2 (eigenvalue 18.6) accounted for 15 % of the variance. Positive loadings > 0.5 (Fig. 4a) corresponded to of a series of carbohydrate products (Subset A, Table 2), and negative loadings to another set of carbohydrates products, N-compounds, toluene, multiple phenolic

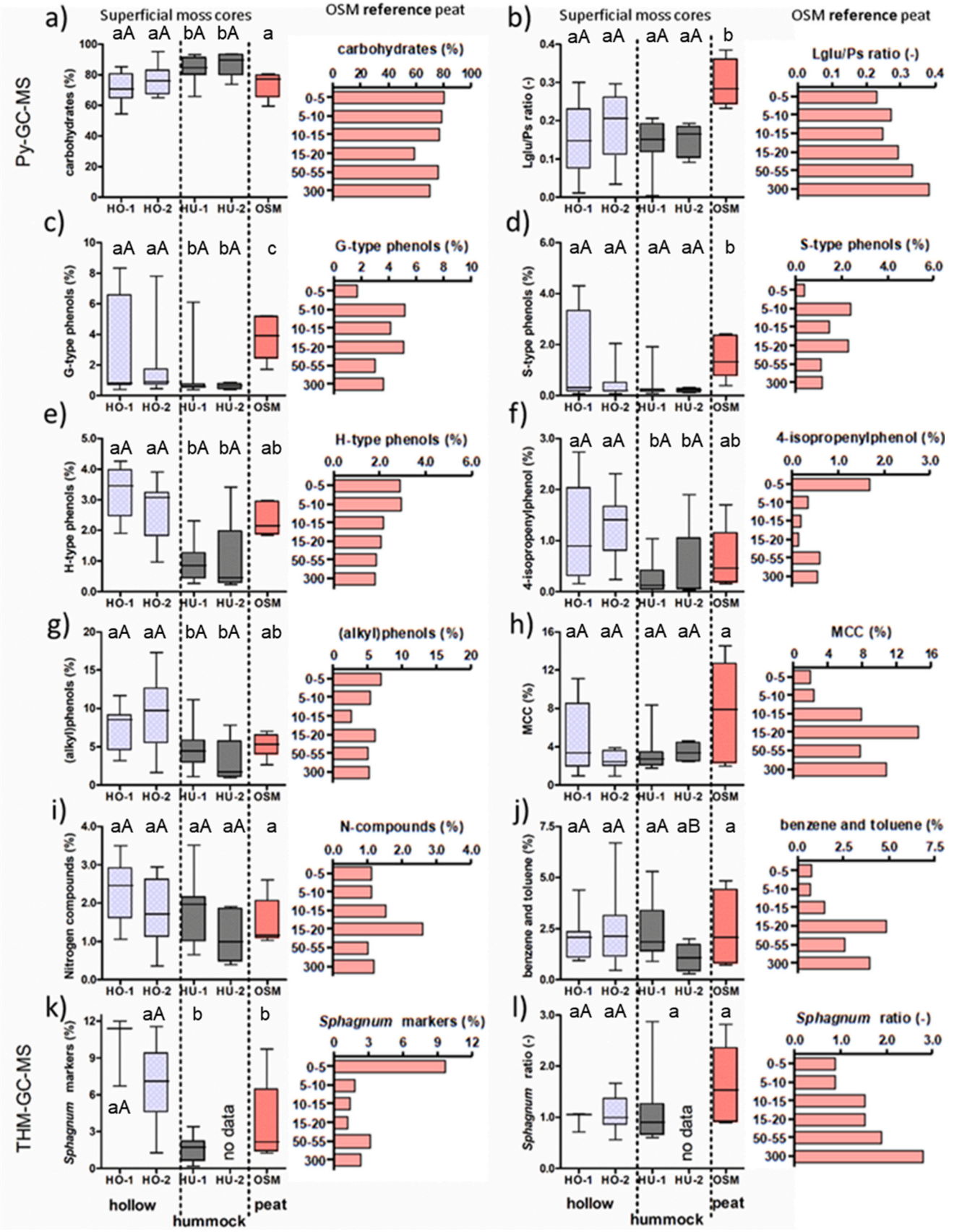

(caption on next page)

Fig. 3. Results from Py-GC-MS (a-j) and THM-GC-MS (k-l), showing boxplots of product group percentages (%) in the superficial moss cores (HO-1 and HO-2 from hollows; HU-1 and HU-2 from hummocks) and the Odersprungmoor peat deposit (OSM), and histograms of trends within the OSM reference peat deposit (numerical ranges indicate depth in cm). a) Carbohydrate products, b) the levoglucosan/total carbohydrates ratio, c) guaiacyl lignin products, d) syringyl lignin products, e) *p*-hydroxyphenyl products, f) 4-isopropenylphenol (*Sphagnum* marker), g) phenol and alkylphenols, h) methylene chain compounds (MCC; aliphatic material), i) nitrogen-containing compounds, j) benzene and toluene, k) sum of *Sphagnum* markers from THM-GC-MS, l) ratio of sphagnum acid decay (4-isopropenylphenol/butenoic acid derivatives). Vertical dotted lines are a visual reference to separate the different types of analyzed cores. Boxplots (box=25–75 % interquartile range; line=median and whiskers indicate the minimum and maximum values) include data from all sample depths and incubation times in each case (Table 1 for number of samples in each core). Letters from the *post-hoc* analyses indicate significant differences ($p < 0.05$): lowercase letters indicate comparisons between the different types of analysed cores (hollow, hummock, and peat-OSM) while uppercase letters indicate comparisons between cores of the same group.

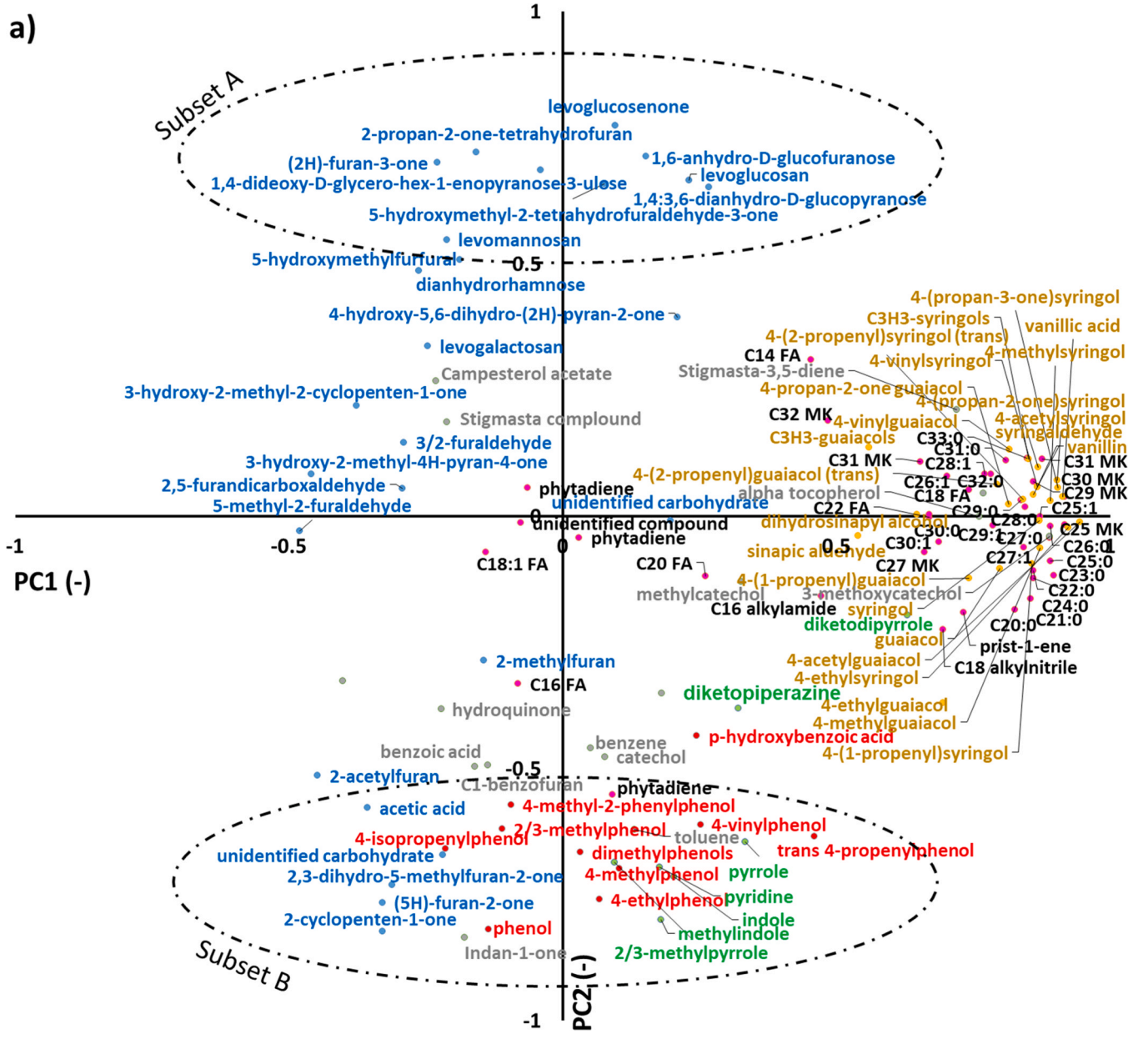

Fig. 4. Results of PCA of the Py-GC-MS dataset. a) PC1-PC2 loadings plot (blue=carbohydrates; red=phenols; yellow=lignin products; black=aliphatic products MCC; green=nitrogen-compounds; grey=other compounds). The MCC are abbreviated as follows: Cxx:0 =alkanes; Cxx:1 =alkenes; FA=fatty acids; MK= 2-methylketones). b) PC1-PC2 scores plot (black=OSM reference peat deposit; red=hummock; blue=hollow; green=reference moss samples). c) Boxplot of PC1 scores for the superficial moss cores and histogram of PC1 scores for the OSM reference peat deposit (depths in cm); d) same as Fig. 3c for PC2. Boxplots (box=25–75 % interquartile range; line=median and whiskers indicate the minimum and maximum values) include data from all sample depths and incubation times in each case (Table 1 for number of samples in each core). Letters from the *post-hoc* analyses indicate significant differences ($p < 0.05$): lowercase letters indicate comparisons between the different types of analysed cores (hollow, hummock, and peat-OSM) while uppercase letters indicate comparisons between cores of the same group.

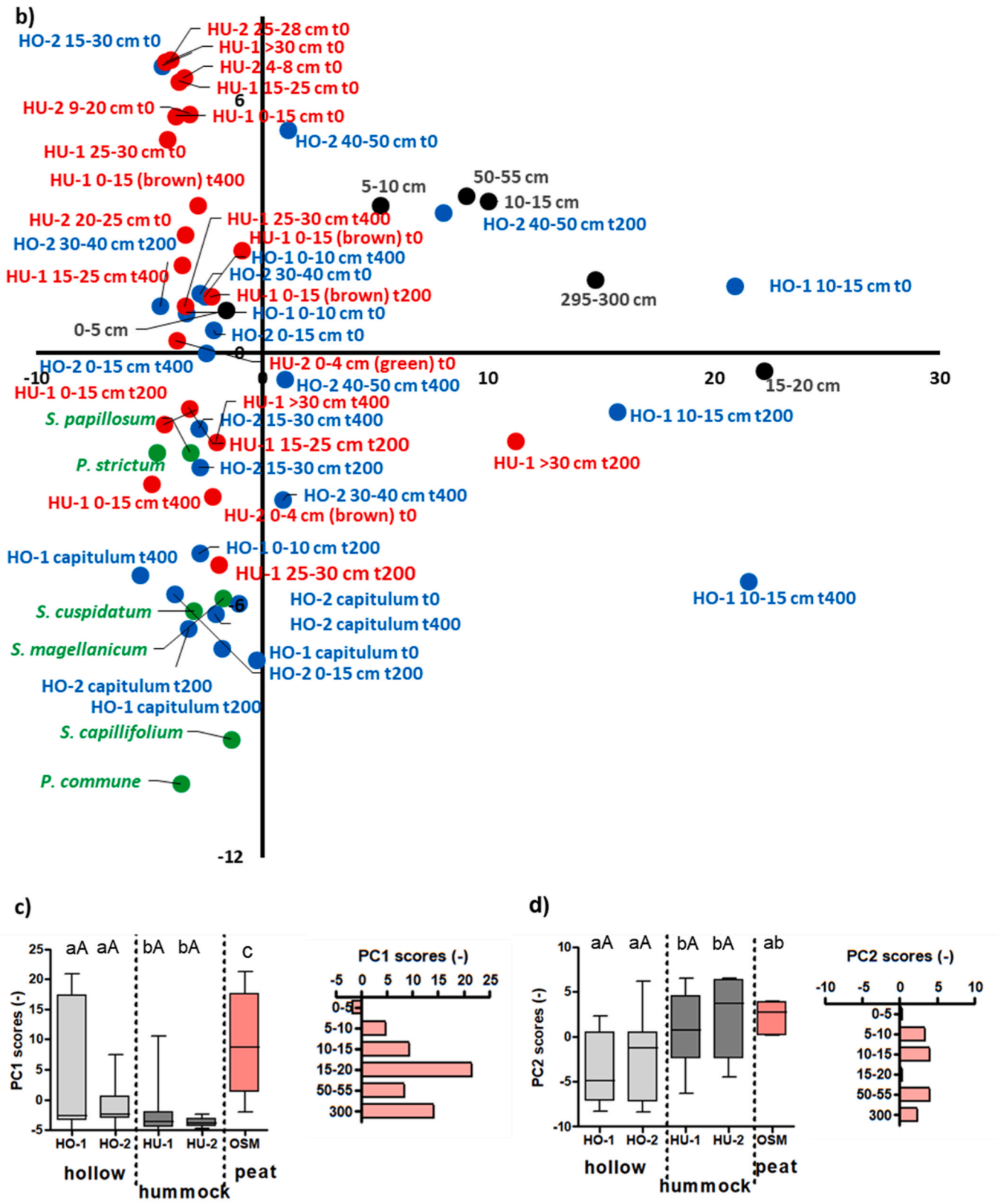

Fig. 4. (*continued*).

compounds including 4IPP and phytadiene (Subset B). Thus, besides the clear moss-derived phenolic OM in Subset B, several products were associated with N-rich moieties in protein and chlorophyll. Most moss and surface core samples were distributed across the PC2 axis with little variation on PC1 (Fig. 4b). The extant moss samples of *Sphagnum*, and *Polytrichum* and the capitulum and green-coloured samples from moss cores (t_0), had negative scores on PC2 whereas the deeper samples at t_0 had positive scores on PC2 (Fig. 4a). Furthermore, the hummock environment was relatively enriched in compounds of Subset A ($P < 0.01$), whereas hollows were enriched in compounds of Subset B ($P < 0.01$)

Table 2
Pyrolysis products associated with the two subsets of compounds identified using PCA. Subset A consists of compounds that have positive loadings > 0.5 and Subset B compounds have negative loadings < -0.5 for PC2.

	Subset A	Subset B
carbohydrates	levoglucosan levoglucosenone 5-hydroxymethylfurfural 5-hydroxymethyl−2-tetrahydrofuraldehyde−3-one 1,4-dideoxy-D-glycero-hex−1-enopyranose−3-ulose (2*H*)-furan−3-one 2-propan−2-one-tetrahydrofuran 1,6-anhydro-β-D-glucofuranose levomannosan 1,4:3,6-dianhydro-α-D-glucopyranose	2-acetylfuran 2-cyclopenten−1-one 2,3-dihydro−5-methylfuran−2-one unidentified carbohydrate acetic acid (5*H*)-furan−2-one
N-compounds		pyridine pyrrole 2/3-methylpyrrole indole methylindole
phenolic compounds		phenol 2/3-methylphenol 4-methylphenol dimethylphenols 4-ethylphenol 4-vinylphenol 4-isopropenylphenol (4IPP) *trans*−4-propenylphenol *p*-hydroxybenzoic acid
Other compounds		toluene phytadiene

(Fig. 4d). The differences between Subset A and Subset B patterns are also illustrated by the example chromatograms of hummock and hollow samples (Fig. 2).

3.3. Effects of incubation on OM composition (mesocosm experiments)

The effects of incubation on Py-GC-MS fingerprints were complex and explored using PCA. The ANOVA revealed a decline in PC2 scores during the first 200 days of incubation, especially in hummocks ($P < 0.05$) (Fig. 5b), whereas for the hollows the difference between t_0 and t_{400} is almost significant ($P = 0.07$) as well. This is consistent with a significant decrease in Subset A compounds and an increase in microbial-derived compounds (N-compounds) from Subset B (Fig. 5c). Furthermore, both hummocks and hollows showed an apparent loss of structural polysaccharides during incubation (evidenced by the Lglu/Ps ratio; Fig. 5d) yet the differences are not statistically significant.

4. Discussion

4.1. Identifying mechanisms: leaching, anaerobic and aerobic decay

The molecular fingerprints of the superficial moss cores from the Odersprungmoor bog were strongly dominated (~80 %) by products of polysaccharides, which is in line with previous studies [25,53]. Their proportion increased during early decay in the field, as evidenced by depth trends within the superficial moss cores. An overall increase in polysaccharides during early decay of *Sphagnum* plants is in agreement with previous studies as well [26,31]. This may indicate the selective preservation of structural polysaccharides including holocellulose and sphagnan, which cannot be distinguished based on the available data. In the light of recent studies, a role of recalcitrant sphagnan seems plausible [54]. On the other hand, another pool of carbohydrates was lost during early decay in the field. We consider it very likely that the clear separation of carbohydrate products along PC2 is indicative of the presence of pools of highly stable (cell wall constituents) and labile (such as hemicellulose [55]) and free or mobile carbohydrates (such as uronic acids). It seems likely that the latter pool is partially present in hyaline cells that are emptied during early decay of *Sphagnum*, i.e. before its remains become part of the peat matrix. We recognize that this assumption is fundamental for our interpretation of the results.

The increase in the PC1 scores from the PCA of the Py-GC-MS data of the OSM peat deposit (from slightly negative values at 0–5 cm to high positive values; Fig. 4c) represents the gradual selective preservation of the more stable lignin and aliphatic OM. This is the typical imprint of anaerobic decay on peat molecular chemistry [26,56]. Anaerobic decay is also significant (high PC1 scores) in bottom samples of the surface moss cores, notably the first peat layer in HO-1 (10–15 cm) with PC1 scores > 20, and is consistent with its black and smeary appearance. The negative scores on PC1 of almost all other samples from the surface moss cores indicate that anaerobic decay is insignificant. In fact, the importance of anaerobic degradation is overrepresented in the PCA due to the extensive homologous series of MCC (e.g. *n*-alkanes and *n*-alkenes), a total of 40 strongly co-varying minor pyrolysis products.

The PC2 is of more interest in this study, as it represents the earliest detectable alteration acting on the moss tissues. All living moss reference materials and green-coloured parts of the superficial moss cores have negative PC2 scores (Fig. 4d), indicating the condition of fresh materials (maintaining the more labile OM and hyaline cell contents). Besides the aforementioned separation of the two main pools of carbohydrates on PC2, pyrolytic markers that decline during early decay (negative on PC2) can be traced to moss-derived phenolics (including sphagnum acid), chlorophyll and N-rich microbial OM. Like the carbohydrates, these constituents may also partition between cell-wall and free pools in the hyaline cells (in cyanobacteria in case of chlorophyll and protein). This corroborates the interpretation of PC2 as indicative of leaching effects during early decay, and selective enrichment of the dominant pool of structural polysaccharides. Further support of a role of leaching is obtained by SEM, which shows clear differences in the physical alteration of the moss samples from green-coloured mosses and moss sections underneath (Fig. 6). Thus, leaching seems to control the variation in OM fingerprint in the superficial moss layers. To the contrary, as discussed in Section 4.3, during incubation experiments the effects of microbial neoformation on OM composition exceed those of leaching in this type of peatland.

The OM alteration parameters PC1 and PC2 allow for some further understanding of early degradation mechanisms. In addition to the transition in carbohydrates fingerprint from a microbial/free pool (negative on PC2) to structural polysaccharides (positive on PC2) (Fig. 4a), the more specific markers of structural polysaccharides such as levoglucosan have highest PC1 loadings. This suggests that not only incipient aerobic decay/leaching (PC2), but also anaerobic decay cause selective preservation of structural polysaccharides over other carbohydrate products. This effect is corroborated by the increase in the Lglu/Ps ratio with depth in the OSM core (Fig. 3b), which has been observed previously in *Sphagnum*-dominated peat [57], including a deep peat core from the Königsmoor bog nearby the study area of the present study (J. Schellekens, pers.comm.). Thus, in *Sphagnum*-dominated peatlands, the Lglu/Ps ratio does not reflect the degree of cellulose alteration (i.e., decreasing Lglu/Ps as decay advances; [31,32]). Instead, it indicates the selective preservation of relatively resistant *Sphagnum*-derived polysaccharides, including cellulose and sphagnan, over hemicellulose and more labile and mobile carbohydrates [57].

Sphagnum acid accumulation in peat deposits depends on the water table, as the compound degrades rapidly under aerobic conditions [25,30,48,53]. Our study shows that sphagnum acid is indeed one of the most labile elements of the peat moss tissue during early decay, affected by leaching and early aerobic decay [31]. Furthermore, the proxy of sphagnum acid decay (Fig. 3l) increases consistently with depth, confirming that decay causes side chain oxidation of remaining sphagnum acid [29,30,58]. Nevertheless, in spite of this long-term alteration and

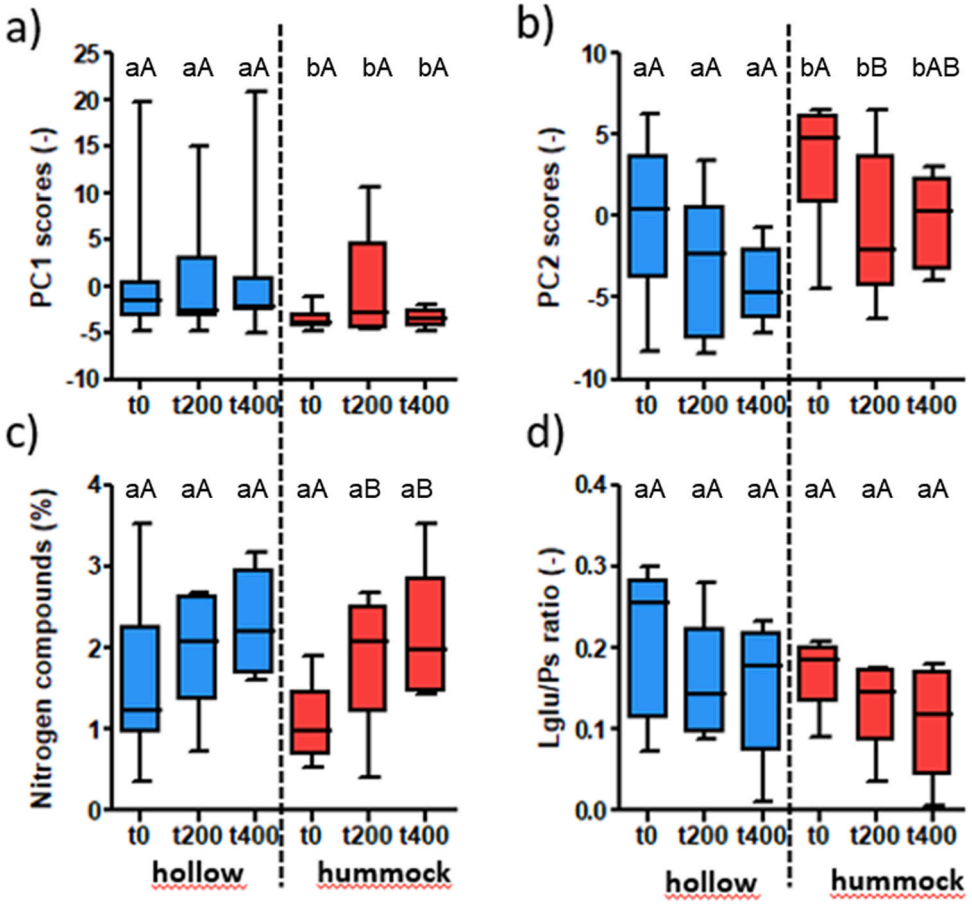

Fig. 5. Effects of incubation treatment (t200 = 200 days, t400 = 400 days) of hollow and hummock samples on selected parameters from Py-GC-MS. a) PC1 scores, indicative of anaerobic decay; b) PC2 scores, indicative of leaching and incipient microbial decay), c) the sum of N-containing compounds (indicative of microbial material formation) and d) the levoglucosan to total carbohydrates products (indicative of polysaccharide preservation degree). Vertical dotted lines are a visual reference to separate the hollow and hummock cores. Boxplots (box=25–75 % interquartile range; line=median and whiskers indicate the minimum and maximum values) include data from all sample depths and incubation times in each case (Table 1 for number of samples in each core). Letters from the *post-hoc* analyses indicate significant differences ($p < 0.05$): lowercase letters indicate comparisons between the different types of analysed cores (hollow and hummock) while uppercase letters indicate comparisons between incubation times. Note the large error bars in PC1 scores of the hollow samples, which is due to high positive values of the highly decomposed deepest sample of the HO-1 moss core (first peat layer).

the rapid depletion of the mobile sphagnum acid pool at the onset of decay, the signal remains detectable on large timescales, indicative of its persistence during long-term anaerobic decay [30]. This validates the markers of sphagnum acid as ideal proxies of specifically leaching and early aerobic decay impact on peat moss [26].

4.2. *Influence of microtopography on sphagnum acid*

4-Isopropenylphenol is often used to reconstruct the past hydrological conditions in peatlands [25,53,57,59,60]. Within the hummock cores, 4IPP levels decrease rapidly from approximately 2–3 % at the surface to below 0.5 % in deeper sections, indicating leaching and perhaps aerobic-favoured decay of sphagnum acid. By contrast, the hollows show elevated 4IPP levels at most depths (Fig. 3f). It is striking that the marker can persist for thousands of years in deep peat layers [26,61] and Pleistocene peat moss [23] within low oxygen systems, yet vanishes rapidly in aerobic environments of hummocks. The high intensity of decay and leaching observed in the hummocks may be related to the aforementioned drought period of 2018 in Europe (and to a lesser extent 2019). This could have caused the loss of hyaline cell contents [62] in spite of hummock vegetation normally being adapted to drier conditions than hollow vegetation [63], for instance by creating higher percentages of hyaline cells [64]. It is possible that the emptying of the hyaline cells during field decay in the hummocks actually represents a rather extreme decomposition event. Therefore, additional molecular-based studies in superficial hummock and hollow habitats in *Sphagnum*-dominated peatland are required, preferably including techniques that can differentiate holocellulose and sphagnan (not Py-GC-MS), to improve our understanding of leaching on OM composition during peat formation.

Although the Py-GC-MS datasets are semi-quantitative, reported maximum sphagnum acid marker 4IPP percentages in literature rarely exceed 3 % [25,53,57]. The fact that 4IPP content is in the range of 0.1–0.5 % in most studies of *Sphagnum*-dominated peat cores analyzed by Py-GC-MS, despite clear evidence of decay-sensitivity, indicates that the sphagnum acid exists in separate labile or mobile [65,66] and more stable cell-bound pools [23]. We predict that the mobile pool is mobilized from the hyaline cells by leaching during initial degradation. On the other hand, the cell wall-bound pool might be well-preserved once buried, leaving the remaining 4IPP signal of 0.1–0.5 % by the time it reaches the low oxygen levels in the catotelm, after which it remains stable. We therefore suggest that any sample with 4IPP levels > 1 % must have been in the hollow condition (and high water-table) in the period between plant mortality and peat formation, and samples with levels below 0.5 % are very likely to have been in the hummock position or a low water table period in the hollow. The results thus indicate that 4IPP does not only depend on general peatland water table fluctuations [59], but also on position in the microrelief.

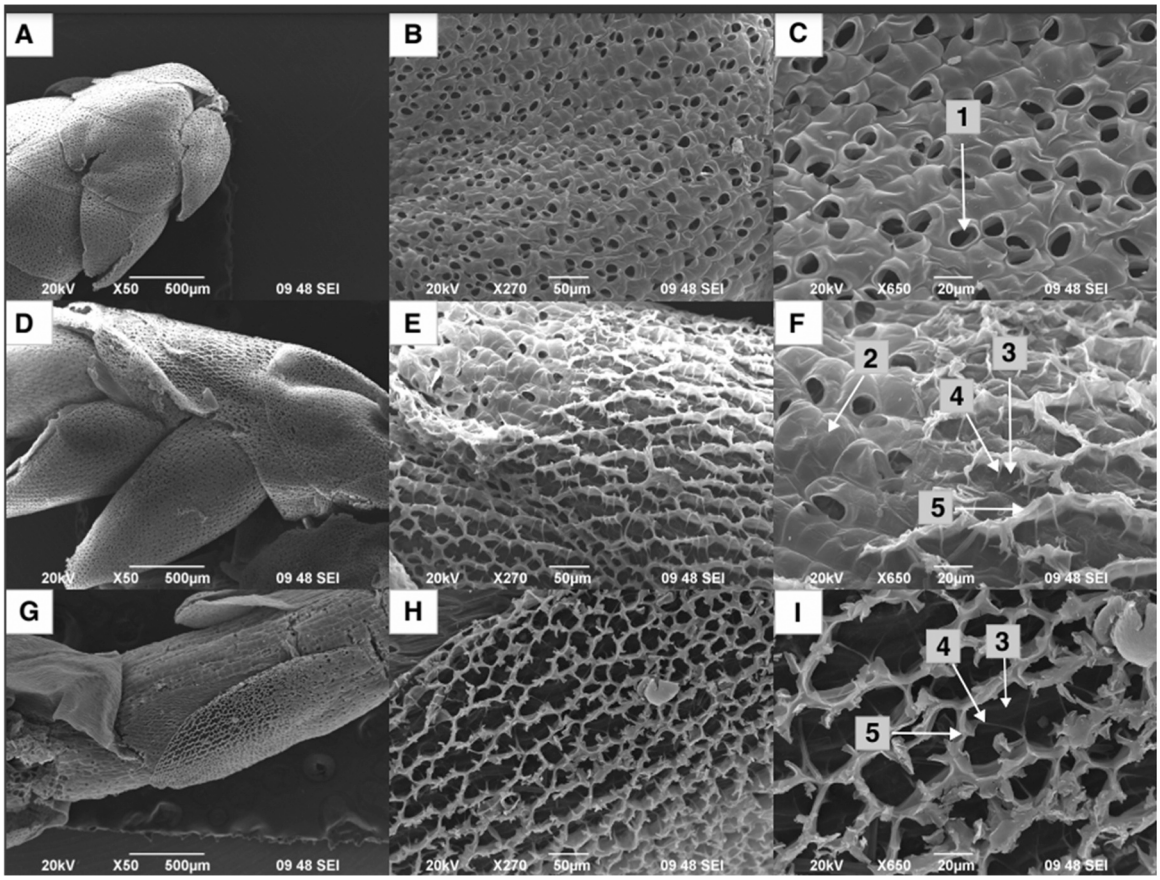

Fig. 6. Scanning electron micrographs of *Sphagnum spp*. at different degradation states from core HO-2. Left columns are a general image of the sample; the middle and right-hand columns correspond to more detailed images of the same section of the sample. (A–C) Spreading branches of photosynthetically active moss (0–15 cm), showing well-preserved hyaline cells and pores. (D– F) Spreading branches of partially degraded *Sphagnum* tissues (15–30 cm) showing coexistence of intact and degraded hyaline cells where most of the cell content has been lost. (G– I) Fragment of stem leaf of partially degraded *Sphagnum* tissues (15–30 cm). Arrows indicate: 1 =pores, 2 =functional (or undamaged) hyaline cells, 3 =damaged hyaline cells, 4 =fibril, 5 = (remains of) chlorophyllose cells.

The hummock-lawn-hollow mosaic can be stable for decades because of feedbacks between vegetation growth, decomposition rates and moisture [67–69]. However, it is unlikely to be stable on timescales relevant for palaeo-ecological reconstructions in temperate peatlands (i.e., centuries to millennia), as microhabitat mosaics have natural fluctuations and shift after disturbance [60,70]. The partial disconnection of 4IPP from variations in *Sphagnum* macrofossils, i.e. notable drops in time-records of 4IPP in periods of stable vegetation composition [32], have been ascribed to a decay-controlled variation, which aligns with our findings, but the underlying mechanism is not necessarily the water table level in the peatland (relevant for climate reconstructions) but also microtopography. Sampling in lawn positions [69], instead of hummocks or hollows, can only partially reduce this effect due to changes in microtopography, urging for multi-core based approaches for water table reconstructions.

4.3. Decay assessment from mesocosm incubation experiments

Our field decay-related observations (based on trends within superficial moss cores and microtopography effects) are not all consistent with the findings from the mesocosms incubation experiments. During the initial 200 days of incubation, there was a decrease in the proportions of the structural polysaccharides pool whereas predominantly microbial-derived compounds showed an increase (Fig. 5), especially in the hummocks. This is also illustrated by a decrease in PC2 scores (Fig. 5). The initial changes include processes that have an opposite effect on some of the molecular markers: microbial neoformation, which generates N-rich OM during laboratory incubation, and leaching, which results in the loss of N-rich OM from bacteria in hyaline cells, in the field. Decay in the mesocosms thus has a partially reverse effect on molecular composition of the OM than early degradation under natural conditions. This may be explained by the lack of a leaching mechanism and higher microbial activity during incubation, the latter of which may be due to the use of a microbial inoculum or the higher temperature in the laboratory than in the field. In fact, the decay effects in the mesocosms are similar to OM decay effects in mineral soils, i.e. N-rich microbial necromass formation and an enrichment in aliphatic compounds in recalcitrant plant-derived OM and microbial OM [71]. Therefore, the mesocosm approach probably did not succeed in mimicking peat decomposition as it occurs in the field. Finally, it is worth stressing that the PCA was crucial in identifying the similarities and differences between decay effects witnessed from the study of original samples vs. those effects during laboratory incubation, reinforcing the particular usefulness of the combination of Py-GC-MS and PCA for the molecular assessment of peat OM [26,56,72].

4.4. Implications for peatland dissolved OM-trace metal linkages

The enrichment factor of THM products from the 0–5 cm to 5–10 cm depth in the OSM peat core and their abundance in experimentally produced water extracts from *Sphagnum* tissues [66] are negatively correlated ($r = -0.58$; $P < 0.001$, Fig. 7). Most compounds with a decline of > 1 % in the OSM peat core surface (this study) have high contributions (>1 %) in the water extracts [66], including all sphagnum acid markers and many other phenolic compounds. Hence, compounds that are lost during early decay+leaching are also the compounds that are

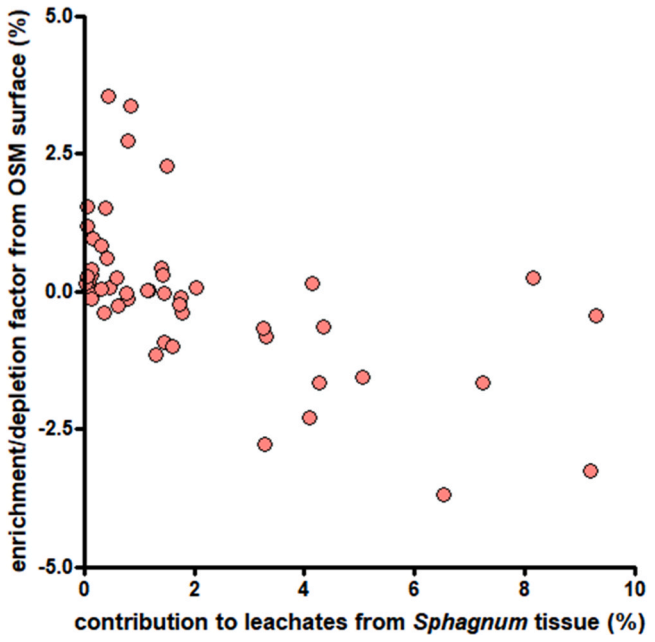

Fig. 7. Dispersion diagram of leachate composition (water extracts) of *Sphagnum* [66] and enrichment (positive)/depletion (negative) factors for THM products from depths of 0–5 cm and 5–10 cm in the OSM peat core (this study). The significant negative linear correlation (r = -0.58; $P < 0.001$) indicates that compounds showing a decline in the OSM peat core are abundant in the leachates. Therefore, molecular constituents that are lost from the solid peat material are susceptible to leaching, supporting an important role of leaching on peat molecular composition during early decay.

enriched in water extracts. No such relationships were found for any other depth interval, suggesting that the leachate chemistry is reflected by the early loss mechanism from the surface peat environment. Furthermore, the main Py-GC-MS products of *Sphagnum*-derived phenols (e.g. 4IPP) were detected in the DOM fraction of brownified Oder stream samples at the outlet of the Odersprungmoor bog studied here (Fig. 1) [29,73] and other bogs in the Harz Mountains [74]. The present study suggests that these compounds originate preferentially from the HU microrelief sections of the bogs, from which they are readily released during early decay, possibly by leaching from hyaline cells. We therefore postulate that the OM-facilitated transport of heavy metals from these historically contaminated peatlands, which is known to be controlled by phenolic DOM [75–77], is driven by leaching from HU microhabitats as well. Hydrological phenomena, such as connectivity of surface and deep peat layers under different moisture regimes, may explain why sphagnum acid is often [29,73,74], but not always [37,78], found in DOM in bog water and streams that drain *Sphagnum*-dominated peatlands. This may be relevant for the management of these areas in the face of environmental change. Targeted research is needed to study the role of the hyaline cells of *Sphagnum* tissues in the biogeochemical processes in *Sphagnum*-dominated peat deposits, its porewater, and adjacent streams.

5. Conclusions

The high proportion of polysaccharides to the OM in this *Sphagnum*-dominated peatland, coupled with the accumulation of structural polysaccharides (including sphagnan) yet the leaching of other carbohydrates, underscores the critical role of polysaccharides in *Sphagnum* in the overall processes of C accumulation and loss within these peatlands. The early-stage alteration of mosses involves the substantial loss from leaching of sphagnum acid, chlorophyll and free carbohydrates, arguably from hyaline cells in *Sphagnum* tissues. These effects are more pronounced in the hummock than in the hollow environment. On the other hand, the hollows are probably more vulnerable to anaerobic decay, i.e. loss of polysaccharides and preservation of lignin and aliphatic OM. This difference probably indicates contrasting decomposition regimes of moss communities, where fast-growing mosses in hollows promote rapid anaerobic decay with no effect on the hyaline cells. Thus, the presence of sphagnum acid in peat cores may be influenced by microrelief position during peat accretion, in addition to water table fluctuations. During laboratory incubation, decay processes are mainly the formation of N-rich microbial OM and degradation of structural polysaccharides, implying a partially reverse effect on molecular fingerprints compared to field decay (leaching). These results advance our understanding of early degradation of peat-forming mosses and the role of microtopography therein.

Funding

Deutsche Forschungsgemeinschaft (DFG) PE 3026/1–1 to M. Pérez-Rodríguez. Slovenian Research Agency program No. P1–0020.

CRediT authorship contribution statement

M. Pérez-Rodríguez: Conceptualization, Methodology, Data curation, Visualization, Writing – original draft, Funding acquisition. **A. Alten:** Writing – review & editing. **M. Miler:** Writing – review & editing. **J. Kaal:** Formal analysis, Data curation, Visualization, Writing – original draft.

Declaration of Competing Interest

The authors declare that there is no conflict of interest.

Acknowledgements

This research was supported by the Deutsche Forschungsgemeinschaft (DFG) PE 3026/1–1 granted to M. Pérez-Rodríguez. We thank Judith Schellekens (Agroscope) for allowing us to contrast the data with that from other peatland cores. From Technische Universität Braunschweig, we are grateful to Harald Biester for helpful discussions, to Adelina Calean, Petra Schmidt and Katja Braun for sample preparation and laboratory analyses, and to Malkin Gerchow for field work assistance. We thank V. Pezdir and M. Gosar (Geological Survey of Slovenia) for assistance with sample preparation for SEM, and Katarzyna Sokołowska and Magdalena Turzańska (University of Wrocław, Poland), Encarnación Núñez Olivera and Javier Martínez Abaigar (Universidad de La Rioja, Spain) for interpretation of SEM micrographs. We are grateful to Monika Koperski for identification of moss species. Last but not least, we are indebted to the reviewers who provided numerous helpful suggestions.

Appendix A. Supporting information

Supplementary data associated with this article can be found in the online version at doi:10.1016/j.jaap.2025.107295.

Data Availability

All data use in this publication is provided in form of figures, tables or supplementary datasets.

References

[1] G. Hugelius, J. Loisel, S. Chadburn, R.B. Jackson, M. Jones, G. MacDonald, M. Marushchak, D. Olefeldt, M. Packalen, M.B. Siewert, C. Treat, M. Turetsky, C. Voigt, Z. Yu, Large stocks of peatland carbon and nitrogen are vulnerable to permafrost thaw, Proc. Natl. Acad. Sci. USA 117 (2020) 20438–20446, https://doi.org/10.1073/pnas.1916387117.

[2] J.E. Kostka, D.J. Weston, J.B. Glass, E.A. Lilleskov, A.J. Shaw, M.R. Turetsky, The *Sphagnum* microbiome: new insights from an ancient plant lineage, N. Phytol. 211 (2016) 57–64, https://doi.org/10.1111/nph.13993.

[3] M.R. Turetsky, The role of bryophytes in carbon and nitrogen cycling, Bryologist 106 (2003) 395–409, https://doi.org/10.1639/05.

[4] H. Rydin, J.K. Jeglum, Oxford. The Biology of Peatlands, 2nd edition, Oxford University Press, 2013, https://doi.org/10.1093/acprof:osobl/9780199602995.001.0001.

[5] S.I. Lang, J.H.C. Cornelissen, T. Klahn, R.S.P. van Logtestijn, R. Broekman, W. Schweikert, R. Aerts, An experimental comparison of chemical traits and litter decomposition rates in a diverse range of subarctic bryophyte, lichen and vascular plant species, J. Ecol. 97 (2009) 886–900, https://doi.org/10.1111/j.1365-2745.2009.01538.x.

[6] T. Hájek, S. Ballance, J. Limpens, M. Zijlstra, J.T.A. Verhoeven, Cell-wall polysaccharides play an important role in decay resistance of Sphagnum and actively depressed decomposition in vitro, Biogeochem 103 (2011) 45–57, https://doi.org/10.1007/s10533-010-9444-3.

[7] L.C. Johnson, A.W.H. Damman, Species-controlled *Sphagnum* decay on a south Swedish raised bog, Oikos 61 (1991) 234, https://doi.org/10.2307/3545341.

[8] L.R. Belyea, Separating the effects of litter quality and microenvironment on decomposition rates in a patterned peatland, Oikos 77 (1996) 529, https://doi.org/10.2307/3545942.

[9] M.R. Turetsky, S.E. Crow, R.J. Evans, D.H. Vitt, R.K. Wieder, Trade-offs in resource allocation among moss species control decomposition in boreal peatlands, J. Ecol. 96 (2008) 1297–1305, https://doi.org/10.1111/j.1365-2745.2008.01438.x.

[10] F. Bengtsson, G. Granath, H. Rydin, Photosynthesis, growth, and decay traits in *Sphagnum* - a multispecies comparison, Ecol. Evol. 6 (2016) 3325–3341, https://doi.org/10.1002/ece3.2119.

[11] M. Mäkilä, H. Säävuori, A. Grundström, T. Suomi, *Sphagnum* decay patterns and bog microtopography in south-eastern Finland (article), Mires Peat 21 (13) (2018) 1–12, https://doi.org/10.19189/MaP.2017.OMB.283.

[12] E.E.S. Ryberg, A. Valdés, J. Ehrlén, M. Väliranta, M.E. Kylander, Quantitative assessment of past variations in *Sphagnum* bog community structure using paleo-species distribution modeling, Ecol 106 (2025) e70033, https://doi.org/10.1002/ecy.70033.

[13] C.G. Laing, G. Granath, L.R. Belyea, K.E. Allton, H. Rydin, Tradeoffs and scaling of functional traits in Sphagnum as drivers of carbon cycling in peatlands, Oikos 123 (2014) 817–828, https://doi.org/10.1111/oik.01061.

[14] T.V. Callaghan, N.J. Collins, C.H. Callaghan, Photosynthesis, growth and reproduction of *Hylocomium splendens* and *Polytrichum commune* in Swedish Lapland. Strategies of growth and population dynamics of tundra plants 4, Oikos 31 (1978) 73, https://doi.org/10.2307/3543386.

[15] N. van Breemen, How *Sphagnum* bogs down other plants, Trends Ecol. Evol. 10 (1995) 270–275, https://doi.org/10.1016/0169-5347(95)90007-1.

[16] J.T.A. Verhoeven, W.M. Liefveld, The ecological significance of organochemical compounds in *Sphagnum*, Acta Bot. Neerl. 46 (1997) 117–130.

[17] A. Bragina, C. Berg, M. Cardinale, A. Shcherbakov, V. Chebotar, G. Berg, *Sphagnum* mosses harbour highly specific bacterial diversity during their whole lifecycle, ISME J. 6 (2012) 802–813, https://doi.org/10.1038/ismej.2011.151. Epub 2011 Nov 17.

[18] D.G. Adams, P.S. Duggan, Cyanobacteria–bryophyte symbioses, J. Exp. Bot. 59 (2008) 1047–1058, https://doi.org/10.1093/jxb/ern005.

[19] Y. Wang, D. Xue, X. Chen, et al., Structure and functions of endophytic bacterial communities associated with *Sphagnum* mosses and their drivers in two different nutrient types of peatlands, Microb. Ecol. 87 (2024) 47, https://doi.org/10.1007/s00248-024-02355-6.

[20] R.S. Clymo, Ion exchange in *Sphagnum* and its relation to bog ecology, Ann. Bot. 27 (1963) 309–324.

[21] T.J. Painter, Man Lindow, Tollund Man and other peat-bog bodies: The preservative and antimicrobial action of sphagnan, a reactive glycuronoglycan with tanning and sequestering properties, Carbohydr. Polym. 15 (1991) 123–142.

[22] A. Von Rudolph, Identifikation der Czapekschen Sphagnolkristalle, Biochem. Physiol. Pflanz. 163 (1972) 110–112.

[23] E. Van der Heijden, J.J. Boon, S. Rasmussen, H. Rudolph, Sphagnum acid and its decarboxylation product isopropenylphenol as biomarkers for fossilised *Sphagnum* in peats, Anc. Biomol. 1 (1997) 93–107.

[24] Y. Zhao, C. Liu, S. Wang, Y. Wang, X. Liu, W. Luo, X. Feng, "Triple locks" on soil organic carbon exerted by sphagnum acid in wetlands, Geochim. Cosmochim. Acta 315 (2021) 24–37, https://doi.org/10.1016/j.gca.2021.09.028.

[25] J. Schellekens, R. Bindler, A. Martínez-Cortizas, E.L. McClymont, G.D. Abbott, H. Biester, X. Pontevedra-Pombal, P. Buurman, Preferential degradation of polyphenols from *Sphagnum* – 4-Isopropenylphenol as a proxy for past hydrological conditions in *Sphagnum*-dominated peat, Geochim. Cosmochim. Acta 150 (2015) 74–89, https://doi.org/10.1016/j.gca.2014.12.003.

[26] J. Schellekens, The use of molecular chemistry (pyrolysis, GC/MS) Environ. Interpret. Peat. PhD Wagening. Univ. (2023) 161.

[27] K. Baumann, Entwicklung der Moorvegetation im Nationalpark Harz, 1st Ed. Aufl. Wernigerode No (2009) 243.

[28] S. Schuldt, A. Buras, M. Arend, et al., A first assessment of the impact of the extreme 2018 summer drought on Central European forests, Basic Appl. Ecol. 45 (2020) 86–103, https://doi.org/10.1016/j.baae.2020.04.003.

[29] J. Kaal, C. Plaza, K.G. Nierop, M. Pérez-Rodríguez, H. Biester, Origin of dissolved organic matter in the Harz Mountains (Germany): a thermally assisted hydrolysis and methylation (THM-GC–MS) study, Geoderma 378 (2020) 114635.

[30] E.Y. Swain, G.D. Abbott, The effect of redox conditions on sphagnum acid thermochemolysis product distributions in a northern peatland, J. Anal. Appl. Pyrol. 103 (2013) 2–7, https://doi.org/10.1016/j.jaap.2012.12.022.

[31] J. Schellekens, P. Buurman, X. Pontevedra-Pombal, Selecting parameters for the environmental interpretation of peat molecular chemistry – a pyrolysis-GC/MS study, Org. Geochem. 40 (2009) 678–691, https://doi.org/10.1016/j.orggeochem.2009.03.006.

[32] E.L. McClymont, E.M. Bingham, C.J. Nott, F.M. Chambers, R.D. Pancost, R. P. Evershed, Pyrolysis GC–MS as a rapid screening tool for determination of peat-forming plant composition in cores from ombrotrophic peat, Org. Geochem 42 (2011) 1420–1435, https://doi.org/10.1016/j.orggeochem.2011.07.004.

[33] R. Development Core Team, R: A Language and Environment for Statistial Computing, 2019. ⟨https://www.r-project.org⟩.

[34] A.D. Pouwels, G.B. Eijkel, J.J. Boon, Curie-point pyrolysis-capillary gas chromatography-high-resolution mass spectrometry of microcrystalline cellulose, J. Anal. Appl. Pyrol. 14 (1989) 237–280.

[35] F. Martin, C. Saiz-Jimenez, F. Gonzalez-Vila, Pyrolysis-gas chromatography-mass spectrometry of lignins, Holzforschung 33 (1979) 210–212.

[36] C. Zaccone, D. Said-Pullicino, G. Gigliotti, T.M. Miano, Diagenetic trends in the phenolic constituents of *Sphagnum*-dominated peat and its corresponding humic acid fraction, Org. Geochem 39 (2008) 830–838, https://doi.org/10.1016/j.orggeochem.2008.04.018.

[37] O. Kracht, G. Gleixner, Isotope analysis of pyrolysis products from Sphagnum peat and dissolved organic matter from bog water, Org. Geochem 31 (2000) 645–654, https://doi.org/10.1016/S0146-6380(00)00041-3.

[38] D.G. Van Smeerdijk, J.J. Boon, Characterisation of subfossil *Sphagnum* leaves, rootlets of Ericaceae and their peat by pyrolysis-high-resolution gas chromatography-mass spectrometry, J. Anal. Appl. Pyrol. 11 (1987) 377–402.

[39] B.A. Stankiewicz, J.C. Hutchins, R. Thomson, D.E.G. Briggs, R.P. Evershed, Assessment of bog-body tissue preservation by pyrolysis-gas chromatography/mass spectrometry, Rapid Commun. Mass Spectrom. 11 (1997) 1884–1890, https://doi.org/10.1002/(SICI)1097-0231(199711)11:17<1884::AID-RCM62>3.0.CO;2-5.

[40] X. Lu, X. Gu, A review on lignin pyrolysis: pyrolytic behavior, mechanism, and relevant upgrading for improving process efficiency, Biotechnol. Biofuels 15 (2022) 106, https://doi.org/10.1186/s13068-022-02203-0.

[41] S. Tsuge, H. Matsubara, High-resolution pyrolysis-gas chromatography of proteins and related materials, J. Anal. Appl. Pyrol. 8 (1985) 49–64.

[42] I. Yassir, P. Buurman, Soil organic matter chemistry changes upon secondary succession in Imperata Grasslands, Indonesia: a pyrolysis-GC/MS study, Geoderma 173-174 (2012) 94–103, https://doi.org/10.1016/j.geoderma.2011.12.024.

[43] D. Fabbri, R. Helleur, Characterization of the tetramethylammonium hydroxide thermochemolysis products of carbohydrates, J. Anal. Appl. Pyrol. 49 (1999) 277–293.

[44] C. Schwarzinger, A. Pfeifer, H. Schmidt, Determination of the nitrogen content of cationic cellulose fibers by analytical pyrolysis, Mon. Chem. 133 (2002) 1–7.

[45] I. Tanczos, C. Schwarzinger, H. Schmidt, J. Balla, THM-GC/MS analysis of model uronic acids of pectin and hemicelluloses, J. Anal. Appl. Pyrol. 68 (2003) 151–162.

[46] C. Estournel-Pélardy, F. Delarue, L. Grasset, F. Laggoun-Défarge, A. Amblès, Tetramethylammonium hydroxide thermochemolysis for the analysis of cellulose and free carbohydrates in a peat bog, J. Anal. Appl. Pyrol. 92 (2011) 401–406.

[47] K. Younes, L. Grasset, Analysis of molecular proxies of a peat core by thermally assisted hydrolysis and methylation-gas chromatography combined with multivariate analysis, J. Anal. Appl. Pyrol. 124 (2017) 726–732, https://doi.org/10.1016/j.jaap.2016.11.014.

[48] G.D. Abbott, E.Y. Swain, A.B. Muhammad, K. Allton, L.R. Belyea, C.G. Laing, G. L. Cowie, Effect of water-table fluctuations on the degradation of *Sphagnum* phenols in surficial peats, Geochim. Cosmochim. Acta 106 (2013) 177–191, https://doi.org/10.1016/j.gca.2012.12.013.

[49] E. van der Heijden, A combined anatomical and pyrolysis mass spectroscopic study of peatified plant tissues, PhD Thesis Univ. Amst. (1994) (The Netherlands).

[50] D. Zak, C. Roth, V. Unger, T. Goldhammer, N. Fenner, C. Freeman, G. Jurasinski, Unraveling the importance of polyphenols for microbial carbon mineralization in rewetted riparian peatlands, Front. Environ. Sci. 7 (2019) 147, https://doi.org/10.3389/fenvs.2019.00147.

[51] P.E. Kolattukudy, Polyesters in Higher Plants, in: W. Babel, A. Steinbüchel (Eds.), Biopolyesters, Springer Berlin Heidelberg, Berlin, Heidelberg, 2001, pp. 1–49, https://doi.org/10.1007/3-540-40021-4_1.

[52] K.G. Nierop, J.M. Verstraten, Rapid molecular assessment of the bioturbation extent in sandy soil horizons under pine using ester-bound lipids by on-line thermally assisted hydrolysis and methylation-gas chromatography/mass spectrometry, Rapid Commun. Mass Spectrom. 18 (2004) 1081–1088.

[53] J. Schellekens, J.A. Bradley, T.W. Kuyper, I. Fraga, X. Pontevedra-Pombal, P. Vidal-Torrado, G.D. Abbott, P. Buurman, The use of plant-specific pyrolysis products as biomarkers in peat deposits, Quat. Sci. Rev. 123 (2015) 254–264, https://doi.org/10.1016/j.quascirev.2015.06.028.

[54] L. Bryan, R. Shaw, E. Schoonover, et al., Sphagnan in *Sphagnum*-dominated peatlands: bioavailability and effects on organic matter stabilization, Biogeochem 167 (2024) 665–680, https://doi.org/10.1007/s10533-024-01134-2.

[55] H. Serk, M.B. Nilsson, J. Figueira, J.P. Krüger, J. Leifeld, C. Alewell, J. Schleucher, Organochemical characterization of peat reveals decomposition of specific hemicellulose structures as the main cause of organic matter loss in the acrotelm, Environ. Sci. Technol. 56 (2022) 17410–17419, https://doi.org/10.1021/acs.est.2c03513.

[56] P. Buurman, K.G.J. Nierop, X. Pontevedra-Pombal, A. Martínez Cortizas, Molecular chemistry by pyrolysis–GC/MS of selected samples of the Penido Vello peat

deposit, Galicia, NW Spain. Developments in Earth Surface Processes, Chapter 10, Elsevier, 2006, pp. 217–240, https://doi.org/10.1016/S0928-2025(06)09010-9.
[57] L. Zeh, M.T. Igel, J. Schellekens, J. Limpens, L. Bragazza, K. Kalbitz, Vascular plants affect properties and decomposition of moss-dominated peat, particularly at elevated temperatures, Biogeosciences 17 (2020) 4797–4813, https://doi.org/10.5194/bg-17-4797-2020.
[58] N. Weiss, J. Kaal, Characterization of labile organic matter in Pleistocene permafrost (NE Siberia), using Thermally assisted Hydrolysis and Methylation (THM-GC-MS), Soil Biol. Biochem 117 (2018) 203–213, https://doi.org/10.1016/j.soilbio.2017.10.001.
[59] T. Kuder, M.A. Kruge, Preservation of biomolecules in sub-fossil plants from raised peat bogs — a potential paleoenvironmental proxy, Org. Geochem 29 (1998) 1355–1368, https://doi.org/10.1016/S0146-6380(98)00092-8.
[60] K. Klein, J. Schellekens, M. Groβ-Schmölders, P. von Sengbusch, C. Alewell, J. Leifeld, Characterizing ecosystem-driven chemical composition differences in natural and drained Finnish bogs using pyrolysis-GC/MS, Org. Geochem 165 (2022) 104351, https://doi.org/10.1016/j.orggeochem.2021.104351.
[61] M.E. Kylander, A. Martínez-Cortizas, R. Bindler, J. Kaal, J.K. Sjöström, S. V. Hansson, N. Silva-Sánchez, S.L. Greenwood, K. Gallagher, J. Rydberg, C.-M. Mörth, S. Rauch, Mineral dust as a driver of carbon accumulation in northern latitudes, Sci. Rep. 8 (2018) 6876, https://doi.org/10.1038/s41598-018-25162-9.
[62] F. Rezanezhad, J.S. Price, W.L. Quinton, B. Lennartz, T. Milojevic, P. Van Cappellen, Structure of peat soils and implications for water storage, flow and solute transport: a review update for geochemists, Chem. Geol. 429 (2016) 75–84, https://doi.org/10.1016/j.chemgeo.2016.03.010.
[63] F. Bengtsson, G. Granath, N. Cronberg, H. Rydin, Mechanisms behind species-specific water economy responses to water level drawdown in peat mosses, Ann. Bot. 126 (2020) 219–230, https://doi.org/10.1093/aob/mcaa033.
[64] Z.-J. Bu, X.-X. Zheng, H. Rydin, T. Moore, J. Ma, Facilitation vs. competition: Does interspecific interaction affect drought responses in *Sphagnum*? Basic Appl. Ecol. 14 (2013) 574–584, https://doi.org/10.1016/j.baae.2013.08.002.
[65] S. Rasmussen, C. Wolff, H. Rudolph, Compartmentalization of phenolic constituents in sphagnum, Phytochem 38 (1995) 35–39, https://doi.org/10.1016/0031-9422(94)00650-I.
[66] J. Kaal, C. Plaza, M. Pérez-Rodríguez, H. Biester, Towards understanding ecological disaster in the Harz Mountains (Central Germany) by carbon tracing: pyrolysis-GC-MS of biological tissues and their water-extractable organic matter (WEOM), Anal. Pyrolysis Lett. 8 (2020) 1–17. ⟨https://pyrolyscience.com/apl008/⟩.
[67] P. Van der Molen, S. Hoekstra, A palaeoecological study of a hummock-hollow complex from Engbertsdijksveen, in the Netherlands, Rev. Palaeobot. 56 (1988) 213–274.
[68] M.K. Nungesser, Modelling microtopography in boreal peatlands: hummocks and hollows, Ecol. Model 165 (2003) 175–207, https://doi.org/10.1016/S0304-3800(03)00067-X.
[69] F.D. Vleeschouwer, F.M. Chambers, G.T. Swindles, Coring and sub-sampling of peatlands for palaeoenvironmental research, Mires Peat 7 (2010) 10.
[70] B.W. Benscoter, R. Kelman Wieder, D.H. Vitt, Linking microtopography with post-fire succession in bogs, J. Veg. Sci. 16 (2005) 453–460, https://doi.org/10.1111/j.1654-1103.2005.tb02385.x.
[71] K. Vancampenhout, K. Wouters, B. De Vos, P. Buurman, R. Swennen, J.A. Deckers, Differences in chemical composition of soil organic matter in natural ecosystems from different climatic regions – a pyrolysis-GC/MS study, Soil Biol. Biochem 41 (2009) 568–579.
[72] H. Biester, K.-H. Knorr, J. Schellekens, A. Basler, Y.-M. Hermanns, Comparison of different methods to determine the degree of peat decomposition in peat bogs, Biogeosciences 11 (2014) 2691–2707, https://doi.org/10.5194/bg-11-2691-2014.
[73] J. Kaal, A. Martínez-Cortizas, H. Biester, Downstream changes in molecular composition of DOM along a headwater stream in the Harz mountains (Central Germany) as determined by FTIR, Pyrolysis-GC–MS and THM-GC–MS, J. Anal. Appl. Pyrol. 126 (2017) 50–61, https://doi.org/10.1016/j.jaap.2017.06.025.
[74] J. Kaal, M. Pérez-Rodríguez, H. Biester, Molecular probing of DOM indicates a key role of spruce-derived lignin in the DOM and metal cycles of a headwater catchment: can spruce forest dieback exacerbate future trends in the browning of Central European surface waters? Environ. Sci. Technol. (2022) acs.est.1c04719 https://doi.org/10.1021/acs.est.1c04719.
[75] J. Buschmann, A. Kappeler, U. Lindauer, D. Kistler, M. Berg, L. Sigg, Arsenite and arsenate binding to dissolved humic acids: Influence of pH, type of humic acid, and aluminum, Environ. Sci. Technol. 40 (2006) 6015–6020, https://doi.org/10.1021/es061057+.
[76] R.A. White, C. Freeman, H. Kang, Plant-derived phenolic compounds impair the remediation of acid mine drainage using treatment wetlands, Ecol. Eng. 37 (2011) 172–175, https://doi.org/10.1016/j.ecoleng.2010.08.008.
[77] E. Neubauer, F. von der Kammer, K.-H. Knorr, S. Peiffer, M. Reichert, T. Hofmann, Colloid-associated export of arsenic in stream water during stormflow events, Chem. Geol. 352 (2013) 81–91, https://doi.org/10.1016/j.chemgeo.2013.05.017.
[78] L. Gandois, A.M. Hoyt, C. Hatté, L. Jeanneau, R. Teisserenc, M. Liotaud, N. Tananaev, Contribution of peatland permafrost to dissolved organic matter along a thaw gradient in North Siberia, Environ. Sci. Technol. 53 (2019) 14165–14174, https://doi.org/10.1021/acs.est.9b03735.